J. Mar. Biol. Ass. U.K. (2006), **86**, 1267–1280
Printed in the United Kingdom
doi: 10.1017/S0025315406014287

Functional relationships and bio-optical properties derived from phytoplankton pigments, optical and photosynthetic parameters; a case study of the Benguela ecosystem

James R. Fishwick*[†¶], Jim Aiken*[†], Ray Barlow[‡], Heather Sessions[‡], Stuart Bernard[ʃ] and Josephine Ras[§]

*Plymouth Marine Laboratory, Prospect Place, Plymouth, Devon, PL1 3DH, UK. [†]Centre for observation of Air–Sea Interactions & fluXes (CASIX). [‡]Marine & Coastal Management, Private Bag X2, Rogge Bay 8012, Cape Town, South Africa. [ʃ]University of Cape Town, Department of Oceanography, Private Bag, Rondebosch 7700, Cape Town, South Africa. [§]Laboratoire d'Océanographie de Villefranche, B.P. 08, 06238, Villefranche-sur-Mer, France.
[¶]Corresponding author, e-mail: J.Fishwick@pml.ac.uk

The relationships between phytoplankton pigments, optical properties and photosynthetic parameters for different phytoplankton functional types (derived by diagnostic pigment indices, DPI) were determined from data acquired in the Benguela ecosystem and the offshore region in October 2002. We observed robust inter-pigment relationships: total chlorophyll-*a* (TChl*a*) was highly correlated with total pigment (TP) and accessory pigment (AP). However, the regression equations for stations dominated by flagellates differed from the equations for stations dominated by diatoms and dinoflagellates. The pigment ratio TChl*a*/TP and the optical ratio a676/a440 were not constant but increased non-linearly with increasing TChl*a* or TP; complimentarily the AP/TP and a490/a676 ratios decreased. There were significant non linear relationships between the photosynthetic parameters F_v/F_m or σ_{PSII} measured by Fast Repetition Rate Fluorometry and TChl*a* or TP. Pigment ratios, optical ratios, F_v/F_m and σ_{PSII} were all inter-correlated with high significance. We determined the distinctive bio-optical properties associated with dominant phytoplankton functional types (derived by DPI) that conformed to the classical partitioning: flagellates (nano-plankton, comprising several taxa) had low biomass, low TChl*a*/TP fraction and low F_v/F_m and high σ_{PSII}; diatoms and dinoflagellates (micro-plankton) had high biomass, pigment ratios, F_v/F_m and low σ_{PSII}.

INTRODUCTION

An understanding of the functional role of plankton in aquatic ecosystems is crucial to quantifying and understanding the Earth system and its role in the regulation of climate. In the marine environment, the organization of plankton, species diversity and seasonal succession are aspects of ecology that differ regionally; knowledge of this diversity is core to understanding phytoplankton functional roles. The environmental conditions (light, nutrients, temperature, salinity, turbulence and stratification) in different ecosystems are the characteristics that force plankton diversity and seasonal succession. Quantifying the Earth system needs representations of marine ecosystems that are realistic, evolving from simple system descriptions (Fasham, 1993) to more complex biomechanistic models (Flynn, 2001) tempered by the realization that not all the hundreds of plankton species can be included explicitly. The use of keystone species or functional types to represent ecosystem functioning is a practical strategy, used by models such as the European Regional Seas Ecosystem Model (ERSEM; Blackford et al., 2004) and the Dynamic Green Ocean Model (DGOM; Le Quéré et al., 2005). For explanation of symbols, abbreviations and acronyms see Table 1.

Global and regional models of primary production (Platt, 1986; Morel, 1991; Behrenfeld & Falkowski, 1997) have used chlorophyll-*a* (Chl*a*) derived from satellite ocean colour data as the principal variable for phytoplankton biomass. Chlorophyll-*a* is both the major ubiquitous light-harvesting pigment and an essential component of plant photo-systems (both PSI and PSII) but it is an inexact proxy for biomass because of the variability of the Carbon:Chl*a* ratio (Geider et al., 1997). The pigment assemblage differs for different phytoplankton taxa, comprising light-harvesting photosynthetic carotenoids (PSCs) and photoprotective carotenoids (PPCs) both of which can be involved in the regulation of the quantum efficiency of photosynthesis. Individual PSCs and PPCs have been used as 'taxa-specific' pigments: e.g. fucoxanthin (PSC) for diatoms; peridinin (PSC) for dinoflagellates; zeaxanthin (PPC) for prokaryotes. These are useful but not definitive indicators. The detection of 'taxa-specific' colour signatures in remotely sensed ocean colour spectra could provide data on the biomass of phytoplankton functional types, for use in models or for validation of model results. The absorption spectra of PSCs and PPCs are different (Bidigare et al., 1990) but generally the 'taxa-specific' PSCs have broadly similar absorption spectra differing only in fine-structure and rendering the bio-optical approach non-specific. There have been

https://doi.org/10.1017/S0025315406014287 Published online by Cambridge University Press

Table 1. *Abbreviations for phytoplankton pigments, pigment formulae, FRRF variables and photosynthetic parameters, optical absorption ratios and model acronyms.*

Symbol	Description	Formula/Units
Chl*a*	Chlorophyll-*a* (plus allomers and epimers)	Also total chlorophyll-*a* Aiken et al., 2004
Chl*b*	Chlorophyll-*b*	
Chl*c*	Chlorophylls-$c_1+c_2+c_3$	
Chlidea	Chlorophyllide-*a*	
DVChl*a*	Divinyl chlorophyll-*a*	
Allo	Alloxanthin	
But	19′-Butanoyloxyfucoxanthin	
Caro	Carotenes	$\beta\beta$-Carotene + $\beta\varepsilon$-Carotene
Diad	Diadinoxanthin	
Diato	Diatoxanthin	
Fuc	Fucoxanthin	
Lut	Lutein	
Hex	19′-Hexanoyloxyfucoxanthin	
Per	Peridinin	
Viol	Violaxanthin	
Zea	Zeaxanthin	
Pras	Prasinoxanthin	
TChl*a*	Total chlorophyll-*a*	Chl*a* + DVChl*a* + Chlidea
AC	Accessory carotenoids	Allo + But + Caro + Diad + Diato + Fuc + Hex + Lut + Per + Viol + Zea
AP	Accessory pigments	AC + Chl*b* + Chlc_1 + Chlc_2 + Chlc_3
TP	Total pigments	TChl*a* + AP
Tpig	TP as used by Aiken et al., 2004	
DP; DPI	Diagnostic Pigments; DP Indices	Allo + But + Chl*b* + Fuc + Hex + Per + Zea
TChl*a*/TP	Total chlorophyll *a* to total pigments	TChl*a*/TP
TChl*a*/AP	Total chlorophyll *a* to accessory pigments	TChl*a*/AP
PSC	Photosynthetic carotenoids	Per + But + Fuc + Hex + Lut + Pras
PPC	Photoprotective carotenoids	Viol + Diad + Allo + Diato + Zea + Caro
PFT	Phytoplankton functional types (e.g. diatoms, dinoflagellates, flagellates or prokaryotes).	
D	Diatom proportion of DP	Fuc/DP
d	Dinoflagellate proportion of DP	Per/DP
F	Nano flagellate proportion of DP, chrysophytes, prymnesiophytes, cryptophytes and chlorophytes	(Allo + But + Chl*b* + Hex)/DP
P	Prokaryote proportion of DP	Zea/DP
M	Mixed, with significant fractions of D, d and F	
F_o	Initial fluorescence before saturation of PSII	Arbitrary units
F_m	Maximum fluorescence after saturation of PSII	Arbitrary units
F_v	Variable fluorescence=(F_m-F_o)	Arbitrary units
F_v/F_m	Maximum photosynthetic quantum efficiency	Unit-less, range 0–1.
σ_{PSII}	Effective absorption cross section of PSII	$\times 10^{-20}$ m^2 photon^{-1}
PSI	Photosystem I	
PSII	Photosystem II	
a676/a440	Ratio of phytoplankton absorption 676 and 440 nm	Unit-less
D443/D665	Optical densities of phytoplankton extracts in 90% acetone at 443 and 665 nm	Unit-less
D480/D665	Optical densities of phytoplankton extracts in 90% acetone at 480 and 665 nm	Unit-less
ERSEM	European Regional Seas Ecosystem Model	Blackford et al., 2004
DGOM	Dynamic Green Ocean Model	Le Quere et al., 2005

reports of ocean colour data interpreted in terms of phytoplankton functional types (PFTs) mostly by empirical approaches (Gregg et al., 2003; Sathyendranath et al., 2004; Alvain et al., 2005) that might be indicative of an unidentified functional link.

Margalef (1967) discussed the organization of plankton, species diversity and productivity, linked to phytoplankton pigments (Chl*a* in relation to carotenoids) and optical properties e.g. D430/D665 (definitions Table 1). He reported that Chl*a* was more quickly synthesized and decomposed than other pigments and responded more rapidly than other pigments to external changes in the opportunity for growth. Pigment composition was a good indicator of the state of populations, since it covered not only taxonomic composition, but also the physiological state of the plankton. The optical ratio increased from the coast to offshore and was particularly low (TChl*a*/TP, high) in estuaries and plankton blooms.

https://doi.org/10.1017/S0025315406014287 Published online by Cambridge University Press

Schluter et al., 1997 and Holmboe et al., 1999 showed that the fraction of carotenoids was greater for nutrient starved cultures (i.e. low TChl*a*/TP). Jeffrey & Hallegraeff, 1980 reported that D480/D665 (approximating to the carotenoid/Chl*a* ratio) was between 2.5 and 3.0 for living cells with higher ratios for older cells. Heath et al., 1990 reported carbon/Chl*a* ratios, D480/D665 absorption ratios and carbon/nitrogen ratios all co-varied, with low values of D480/D665 ratio, corresponding to high Chl*a*/carotenoid, high Chl*a*/Carbon and high Nitrogen/Carbon, i.e. healthy (photosynthesizing) cells.

In a seasonal study in the western English Channel Aiken et al., 2004 showed that TChl*a*/TP increased from a minimum value ($\sim$0.43) in mid-winter to a maximum in the peak of the spring bloom ($\sim$0.61) and diminished from a secondary maximum in the peak of the autumn bloom ($\sim$0.65) to the mid-winter minimum; in both periods the TChl*a*/TP was linearly correlated with integrated photon flux (PAR) for the previous few days. In the summer stratified period with nutrient depletion in the surface layer, the TChl*a*/TP ratio was low, except in mini-blooms, associated with episodic nutrient pulses, possibly from sub-thermocline sources. There were direct linear relationships between pigment ratios (e.g. TChl*a*/TP) optical ratios (e.g. a676/a443) and photosynthetic quantum efficiency (F_v/F_m) measured by Fast Repetition Rate Fluorometry (FRRF; Kolber & Falkowski, 1993; Kolber et al., 1998). Aiken et al. (2004) concluded that phytoplankton synthesize Chl*a* preferentially to other pigments in conditions beneficial for growth; i.e. the TChl*a*/TP ratio was greater when plants were growing actively and conversely the ratio of AP/TP decreased. Other observations of pigments, optical and photosynthetic parameters derived by FRRF (F_v/F_m and the cross section of PSII, σ_{PSII}, $10^{-20}\,m^2\,photon^{-1}$) have shown similar inter-correlations (e.g. Aiken et al., 2000; Suggett et al., 2001, 2006; Moore et al., 2003, 2005; Aiken et al., 2004; Smyth et al., 2004). The iron enrichment experiments, IronEx II (Behrenfeld et al., 1996) and SOIREE (Boyd & Abraham, 2001) pioneered the use of the FRRF, showing links between F_v/F_m and phytoplankton pigments. Globally, TChl*a*/TP varies from $\sim$0.2 in nutrient (and Fe) depleted zones to $>$0.7 in high-biomass blooms, with F_v/F_m ranging $\sim$0.2–0.65; 0.23–0.55 in IronExII and 0.37–0.53 in the English Channel.

In this paper we analyse the bio-optical data acquired during a two week cruise in the Benguela ecosystem, between Cape Town and the Orange River, from 4–18 October 2002, (station locations Figure 1). Chlorophyll-*a* concentrations were $>25\,mg\,m^{-3}$ in the upwelling zone and $\sim0.25\,mg\,m^{-3}$ in surface water offshore. We test the hypothesis derived from Margalef, 1967 and Aiken et al., 2004: phytoplankton synthesize Chl*a* preferentially to other pigments in conditions conducive to growth, with changes in the phytoplankton community composition as a consequence. In this case study, we analyse the relationships between pigment composition (HPLC pigment analysis) optical absorption spectra and phytoplankton photosynthetic parameters (by FRRF). Together these define the bio-optical properties of the major phytoplankton functional types (PFTs) as determined by diagnostic pigment indices (DPI).

Benguela ecosystem, South Africa

Upwelling in the southern Benguela can be highly variable though a frontal zone is usually well defined in both temperature and pigment distributions, coinciding with the shelf edge. Maximum upwelling occurs in summer (October–March) in the south (33°–34°S) but can be continuous in some 'cells' (Hardman-Mountford et al., 2003). Phytoplankton communities are generally dominated by diatoms and dinoflagellates, but occasionally small flagellates (Mitchell-Innes & Winter, 1987; Pitcher et al., 1992). Diatoms tend to dominate inshore in nutrient-rich water, while flagellates are more important offshore on the seaward side of the fronts. Red tide blooms occur throughout the region, particularly during quiescent periods in aged upwelled water, as stratification increases (Pitcher et al., 1998).

MATERIALS AND METHODS

Temperature, salinity, nutrient and pigment analysis

Station oceanographic properties were measured with a SeaBird Electronics (SBE) 911 Plus CTD in combination with a rosette sampler to collect seawater samples at discrete depths. Nutrient samples were stored at -35°C for analysis ashore using a Technicon Auto-analyser according to Grasshoff et al., 1983 and Kirkwood, 1994. Seawater (0.5–2.0 l) was filtered through 25 mm GF/F filters and frozen immediately in liquid nitrogen for HPLC analysis ashore, using the methods reported by Barlow et al., 1997 and Barlow et al., 2004. Diagnostic pigment indices (Vidussi et al., 2001) were derived to determine the dominant phytoplankton taxonomic groups or functional types (PFTs), as defined in Table 1. Four dominant PFTs were determined: diatoms (D), dinoflagellates (d), small flagellates comprising chrysophytes, prymnesiophytes, cryptophytes and chlorophytes (F) and prokaryotes comprising cyanobacteria and prochlorophytes (P).

Fast repetition rate fluorometer (FRRF)

A Chelsea Technologies Ltd FAST*tracka* (Ser. no. 182043) was deployed from the crane on the starboard quarter (outboard reach 4–6 m) positioned stern-to-sun to avoid ship shadow. The instrument was mounted horizontally with a depth sensor and 2π PAR (400–700 nm) sensor and lowered at $\sim0.5\,m\,s^{-1}$ through the water column to a depth $>$1% light level. The excitation source was a bank of LEDs with peak emission at 478 nm, configured for 100 saturation flashes of duration 1.1 μs with 2.8 μs interval between flashes. The fluorescence signal was detected at 668 nm; 8 sequences were averaged per acquisition. The instrument gain was fixed at 1 for the high chlorophyll inshore stations which prevented data loss due to gain switching and was set to auto-ranging at the offshore stations due to the low signals in the surface waters. Blanks of 0.2 μm filtered seawater were run daily in both the light and dark chambers at all gains (Cullen & Davis, 2003). All data were processed using FRS software (Chelsea Technologies Ltd). No blank corrections were applied as the blank signals constituted less than 1% of the fluorescence at the inshore stations and 5% at the

https://doi.org/10.1017/S0025315406014287 Published online by Cambridge University Press

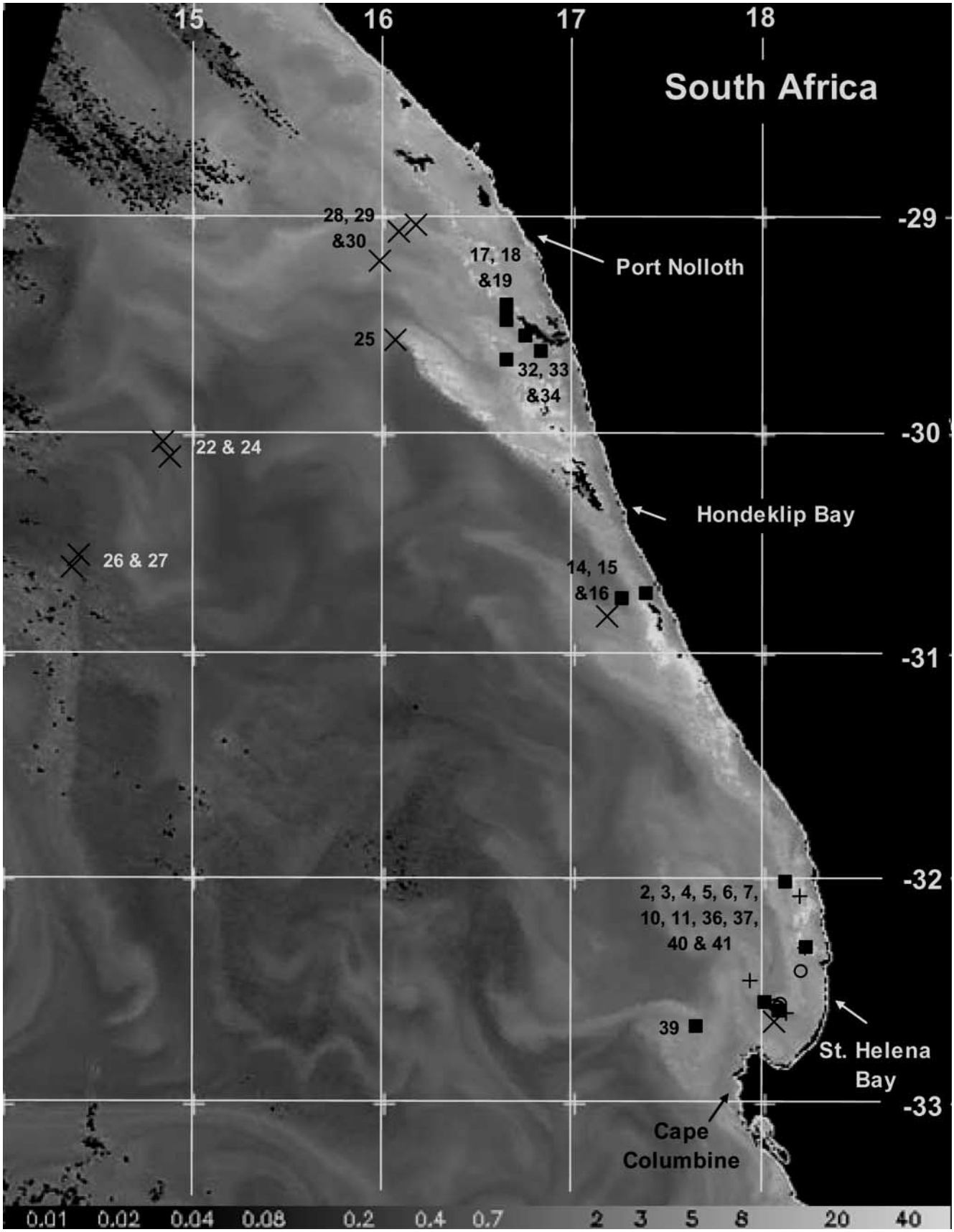

Figure 1. MERIS Chlorophyll (scale bar along the bottom in mg m^{-3}) for 15 October 2002, of the Benguela ecosystem off the west coast of South Africa, showing the station number with the dominant phytoplankton type. Black squares, diatoms; open circles, dinoflagellates; crosses, flagellates; and plus-signs indicate stations with mixed populations.

https://doi.org/10.1017/S0025315406014287 Published online by Cambridge University Press

lowest chlorophyll station offshore. There were 47 FRRF profiles at 37 of the 41 stations. We have focused on the unquenched values of F_v/F_m and σ_{PSII} derived at depths where both photochemical and non-photochemical quenching were negligible and the values of the photosynthetic parameters were maximal (as described in Aiken et al., 2004). The data was binned at 1 m intervals and an average was taken around the maximum unquenched values of F_v/F_m and σ_{PSII}. At a few stations in shallow surface layers or very high light, quenching of F_o and F_m persisted through the surface layer and it was not possible to determine a valid unquenched value for F_v/F_m and σ_{PSII}.

Particulate absorption spectra (PABS)

At each sample depth, a predetermined volume of seawater was filtered through a Whatman GF/F glass-fibre filter. The optical densities of the particles were measured using a LI-COR radiometer (LI-1800 UW) equipped with an integrating sphere. Hydrated GF/F filters were periodically used as a blank. The spectral absorption coefficient of particulate matter, $a_p(\lambda)$, was recorded between 370–750 nm in 2 nm increments. The value of $a_p(750)$ should be equal to zero, so the remaining a_p values were shifted at all wavelengths so $a_p(750)=0$. The path length amplification due to multiple scattering inside the filter was corrected using a parameterization given by Mitchell & Kiefer, 1988. Duplicate filtrations were taken in a non-systematic manner. One filter was soaked in CH_3OH to de-pigment the sample (Kishino et al., 1985) and determine the absorption spectrum of bleached cells and detritus. When the bleaching protocol was not used, the a_p spectrum was de-convolved into its algal and detrital components (a_{ph} and a_d,) by the method of Bricaud & Stramski, 1990.

RESULTS

Physical-biological structures, bio-optical distributions and diversity

The mean data for the surface layer at each station are given in Table 2 and the bio-optical properties for the depths of the unquenched value of F_v/F_m are given in Table 3. In the inshore upwelling zones (see Figure 1) most stations had a surface layer depth of 10 to 20 m but <10 m at three shallow coastal stations. Surface

Table 2. *Average values of surface layer properties: surface layer depth (SLD), temperature (SLT), nitrate concentration, TChl*a*, AP, the dominant phytoplankton type (%, see Table 1), TChla/TP and a676/a440.*

Station	SLD (m)	SLT (°C)	Nitrate (μM)	TChl*a* (mg m^{-3})	AP (mg m^{-3})	Dom. Taxa	Diat (%)	Dino (%)	Flag (%)	Prok (%)	TChl*a*/ TP	a676/ a440
2	12	15.3	0.97	2.01	1.52	F	30	9	54	7	0.569	0.302
3	24	15.1	1.11	3.41	2.94	M	28	34	33	5	0.538	0.342
4	11	16.0	0.14	2.81	2.25	D	42	30	24	4	0.556	0.336
5	21	15.3	0.14	4.04	3.22	d	25	47	24	4	0.556	0.377
6	28	14.7	2.72	6.05	4.26	D	64	23	12	1	0.587	0.458
7	15.5	14.8	0.90	6.41	5.02	d	30	61	7	2	0.561	0.480
8	8	15.2	0.22	9.71	7.44	d	24	69	6	1	0.566	0.494
10	15	15.0	0.93	6.74	4.96	M	46	42	11	1	0.576	0.462
11	20	15.0	0.57	5.92	4.99	d	25	68	4	3	0.543	0.401
12	12	15.2	2.52	4.58	5.06	M	30	32	34	4	0.475	0.406
14	20	13.7	6.36	6.91	5.30	D	53	8	36	3	0.566	0.441
15	10	12.2	23.23	3.01	2.09	D	62	8	28	2	0.591	0.425
16	18	11.5	1.07	2.56	2.41	F	24	15	48	13	0.515	0.354
17	20	15.1	2.68	22.65	14.86	D	84	6	9	1	0.604	
18	15	13.6	5.09	13.06	8.85	D	63	15	21	1	0.596	0.476
19	15	14.4	2.18	24.60	15.08	D	85	5	9	1	0.620	0.582
22	50	16.3	1.07	0.68	0.73	F	11	4	83	2	0.484	0.249
24	36	15.9	1.25	0.58	0.64	F	10	3	84	3	0.476	0.296
25	23	16.1	0.36	0.74	0.85	F	10	14	60	16	0.465	0.232
26	20	16.5	0.36	0.32	0.40	F	18	3	65	14	0.448	0.138
27	10.5	17.0	0.61	0.26	0.30	F	14	3	63	20	0.464	0.166
28	25	16.4	0.41	1.91	2.12	F	24	6	61	9	0.475	0.259
29	23	16.2	0.16	1.71	1.81	F	18	12	62	8	0.485	0.274
30	20	16.3	0.29	1.55	1.65	F	16	14	63	7	0.484	0.262
32	22	14.6	2.10	6.31	5.91	M	46	16	35	3	0.517	0.381
33	21	13.4	4.55	15.67	10.83	D	74	9	16	1	0.591	0.550
34	16	13.3	6.66	18.91	11.99	D	93	1	6	0	0.612	0.616
36	20	15.1	4.21	5.27	4.76	D	70	14	14	2	0.526	0.507
37	11.5	15.8	8.07	3.10	2.78	M	30	23	26	21	0.527	0.387
39	8	16.1	0.14	2.55	2.05	D	50	10	31	9	0.554	0.377
40	10	15.8	0.14	4.11	3.22	D	47	19	24	10	0.560	0.370
41	7	16.1	0.24	8.14	6.76	d	16	77	5	2	0.547	0.443

https://doi.org/10.1017/S0025315406014287 Published online by Cambridge University Press

Table 3. *Summary of the data set taken from the depth of the maximum F_v/F_m: depth of F_v/F_m maximum (DFmax), temperature, nitrate concentration, TChl*a*, AP, the dominant phytoplankton taxa (%, see Table 1), TChl*a*/TP, a676/a440, F_v/F_m and σ_{PSII} ($\times 10^{-20}$ m^2 photon^{-1}).*

Station	DFmax (m)	Temp (°C)	Nitrate (μM)	TChl*a* (mg m^{-3})	AP (mg m^{-3})	Dom. Taxa	Diat (%)	Dino (%)	Flag (%)	Prok (%)	TChl*a* /TP	a676/ a440	F_v/F_m	σ_{PSII}
2	25	14.5	1.79	6.35	3.97	D	62	22	14	2	0.616	0.492	0.570	380
4	16.5	15.3	0.14	4.33	3.62	d	30	50	18	2	0.545	0.400	0.515	460
5	21	14.8	0.14	4.86	3.39	d	30	44	23	3	0.589		0.505	470
6	10.5	14.8	1.93	6.62	4.91	D	60	23	14	3	0.574		0.570	370
7	11	14.8	0.50	7.40	5.87	d	29	63	6	2	0.558	0.549	0.570	360
8	8	15.1	0.17	8.91	6.42	d	27	65	7	1	0.581	0.494	0.565	360
10	7	15.0	0.14	6.72	5.08	M	44	42	12	2	0.570	0.466	0.560	405
11	10	15.0	0.29	5.74	4.99	d	25	64	8	3	0.535	0.501	0.560	350
14	3	13.7	6.26	7.26	5.74	D	52	8	38	2	0.558	0.441	0.510	470
15	18	12.1	22.62	1.72	1.30	D	58	11	29	2	0.570		0.550	380
16	10	11.6	1.14	2.55	2.45	F	23	15	48	14	0.510		0.450	525
22	9.5	16.5	0.86	0.72	0.76	F	12	5	81	2	0.485		0.455	600
24	3	16.2		0.61	0.65	F	11	4	81	4	0.483	0.296	0.400	640
25	23	15.9	0.57	1.04	1.21	F	11	18	67	5	0.460		0.440	585
26	40	15.9	0.42	0.38	0.47	F	16	0	80	4	0.448		0.310	700
27	30	16.1	1.21	0.38	0.48	F	23	3	63	11	0.438		0.250	720
30	27	15.2	1.13	1.55	1.66	F	31	17	47	5	0.483		0.460	575
32	4	14.6	1.84	6.41	6.02	M	44	19	34	3	0.516	0.387	0.460	520
36	10.5	15.1	2.50	7.48	5.54	D	70	15	14	1	0.575		0.545	390
39	3	16.1	0.14	2.71	2.22	D	49	12	31	8	0.550	0.377	0.515	460
41	7	16.2	0.34	9.80	7.95	d	21	74	4	1	0.552	0.443	0.565	350

Table 4. *Regression statistics for the pigment relationships.*

Independent variable	Dependent variable	Group	Type of relationship	Slope	Intercept	R^2	N
TChl*a*	TP	All	Linear	1.621	0.785	0.997	32
TChl*a*	TP	Flag.	Linear	1.901	0.133	0.987	10
TChl*a*	TP	D, d & M	Linear	1.595	1.147	0.997	22
TChl*a*	AP	All	Linear	0.621	0.785	0.981	32
TChl*a*	AP	Flag.	Linear	0.901	0.133	0.942	10
TChl*a*	AP	D, d & M	Linear	0.595	1.147	0.980	22
TP	AP	All	Linear	0.385	0.465	0.993	32
TP	AP	Flag.	Linear	0.481	0.052	0.984	10
TP	AP	D, d & M	Linear	0.375	0.693	0.992	22

temperatures ranged from 11.5°C to 16°C inshore, with the lowest values near the coast where strong upwelling had occurred. Nitrate levels at these stations were generally $>1\,\mu$M, exceeding $22\,\mu$M at Station 15 (12.2°C) and $<0.2\,\mu$M at only five stations in St Helena Bay. Silicate was never $<2.8\,\mu$M at any inshore station. All the inshore stations had surface plankton populations (no sub-surface maximum) though there was evidence of layering at a few stations. The offshore stations, just off-shelf at 16°E (29°S to 29.5°S) and in very deep water 250 km to the west (15°E to 14.4°E) had surface layer depths >20 m above a sub-surface chlorophyll maximum in the thermocline at ~40–50 m. Surface temperatures were higher (16°C to 17°C) with nitrate values 0.2 to $1.25\,\mu$M; again silicate was not depleted ($>1.7\,\mu$M).

Figure 2 shows the surface layer properties arranged by increasing TChl*a* showing the correlated distributions of all the bio-optical properties: increasing pigment ratios (TChl*a*/TP, TChl*a*/AP, Figure 2B) and optical ratios (a676/a440, a676/a490, Figure 2E); the dominance by diatoms at very high TChl*a* (>13 mg m^{-3}; Figure 2C) and flagellates at low TChl*a* (<2.0 mg m^{-3}; Figure 2D) with diatoms, dinoflagellates or mixed populations in the intermediate range 2–10 mg m^{-3}; an increase of F_v/F_m and decrease of σ_{PSII} with increasing TChl*a* (Figure 2F). The TChl*a* was highest (13–25 mg m^{-3}) for Stations 17, 18, 19, 33 and 34, which were all located in the northern-most inshore waters at 29° to 30°S. All were D-dominated (70 to >80%) with the highest values of pigment ratios (>0.6) and optical ratios (0.48–0.62); the FRRF was saturated for these stations so there were no valid data for F_v/F_m and σ_{PSII}. The remaining high TChl*a* stations (2–10 mg m^{-3}) located in St Helena Bay or south of Hondeklip Bay (Stations 2 to 16, 32 and 36 to

https://doi.org/10.1017/S0025315406014287 Published online by Cambridge University Press

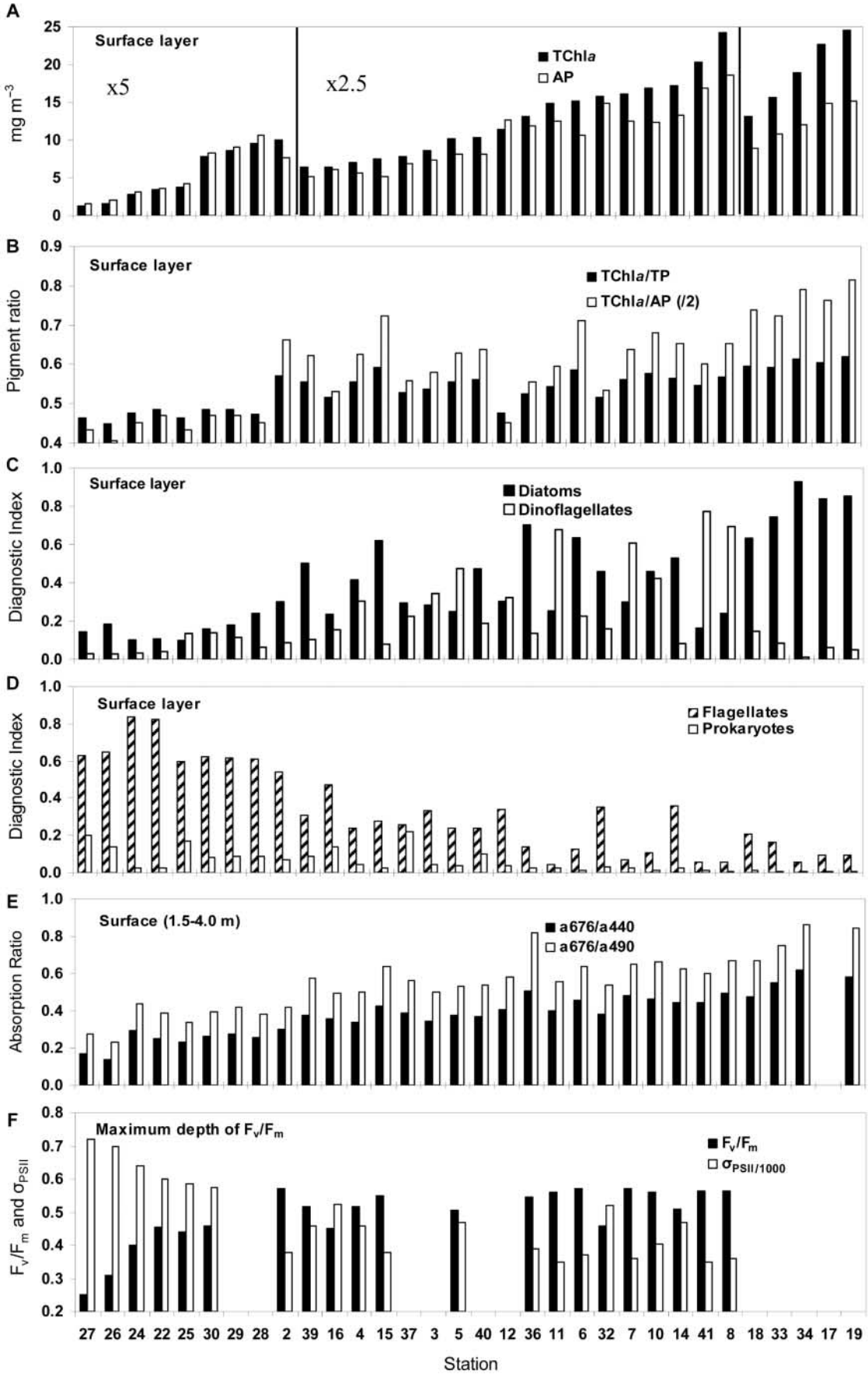

Figure 2. The spatial distribution and diversity (surface layer) by station ranked with increasing chlorophyll-*a* of: (A) TChl*a* and AP, data in the first section is multiplied by 5, in the second section by 2.5 and actual values in the third section; (B) TChl*a*/TP and TChl*a*/AP (divided by 2); (C) DPI for diatoms and dinoflagellates; (D) DPI for flagellates and prokaryotes; (E) optical ratios a676/a440 and a676/a490; (F) maximum (unquenched) values of the photosynthetic parameters F_v/F_m and σ_{PSII} ($\times 10^{-20}$ m^2 photon^{-1}) divided by 1000; all biomass data (pigment concentrations) are in units of mg m^{-3} and all ratios are unit-

https://doi.org/10.1017/S0025315406014287 Published online by Cambridge University Press

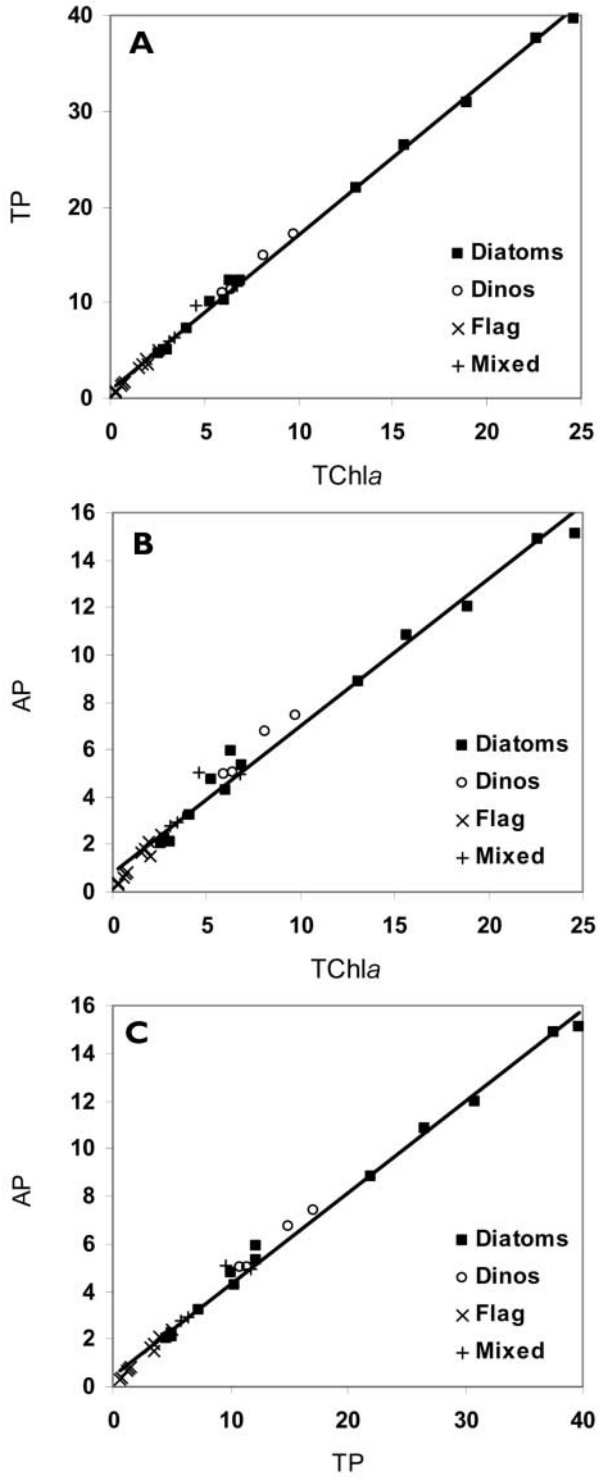

Figure 3. Relationships between (A) TChl*a* versus TP; (B) TChl*a* versus AP; and (C) TP versus AP, all concentrations in mg m^{-3}. The data points on each figure are identified by the dominant taxa at that station and the corresponding regression statistics are given in Table 4.

41) were either D-dominated or d-dominated with some mixed (M) populations; all had moderately high values of pigment ratios (0.48–0.58), optical ratios (0.3–0.55) and F_v/F_m (0.51–0.57) but the lowest values of σ_{PSII} (350–460). The offshore Stations 22 to 30 had the lowest chlorophyll levels (<2 mg m^{-3}) and were all F-dominated (60% to >80%) with the lowest values of pigment ratios (0.44–0.49) optical ratios (0.13–0.3) and F_v/F_m (0.25–0.46) and the highest values of σ_{PSII} (575–720). The TChl*a* was greater than AP for all the high TChl*a* stations, but less than AP in the low TChl*a*, F-dominated stations offshore. Prokaryotes (P) were never the major phytoplankton group, though they constituted 2–20% of the assemblage at most offshore stations (all F-dominated).

Bio-optical relationships

Figure 3 shows the relationships between TChl*a* vs TP (Figure 3A), TChl*a* vs AP (Figure 3B) and TP vs AP (Figure 3C) for the surface layer data from Table 2; the data points are marked with the dominant PFT in the assemblage. The regression statistics (Table 4) show that there was high correlation between TP and TChl*a* for all data ($R^2=0.997$) yet the F-dominated station data, in the low-biomass region of each relationship had a higher slope than the data for the combined mixed, D- and d-dominated assemblages. This observation that diatoms and dinoflagellate populations have a greater fraction of TChl*a* than flagellate populations, or that flagellate populations have a greater fraction of AP, is novel to our knowledge.

The TChl*a*/TP ratio varied from 0.44 to 0.62 with a log relationship to TChl*a* (Figure 4A; Table 5; $R^2=0.71$) having the ratio lowest at low TChl*a* or TP (not shown) for the stations with flagellate dominance and the ratio highest for high TChl*a* (or TP) in mixed, diatom and dinoflagellate dominant populations. The separate regression for the flagellate and others group (M+D+d) showed distinctly different linear relationships (different slopes) with either TChl*a* or TP as the independent variable (Table 5). The relationships between TChl*a* or TP (not shown) and the optical ratios a676/a440 or a676/a490 (not shown) (Figure 4C, $R^2=0.88$) were non-linear and of similar functional form (log) to pigment ratios, with flagellates dominant at low TChl*a* (or TP) and low a676/a440; here the separate regressions for the flagellate group and the others were non-linear (log) with a high fraction of variance explained. The TChl*a* had an inverse relationship to the pigment fraction AP/TP and the optical analogue a490/a676 (Figure 4B,D; $R^2=0.71$ and $R^2=0.79$) with flagellates dominant at high values of AP/TP and a490/a676. The photosynthetic parameters F_v/F_m (Figure 4E, $R^2=0.75$) and σ_{PSII} (inversely, Figure 4F, $R^2=0.80$) were log correlated with TChl*a* at the low TChl*a* flagellate dominated stations, low F_v/F_m and high σ_{PSII} and the reverse for the remnant populations (M, D and d-dominated).

The photosynthetic parameters F_v/F_m and σ_{PSII} were inversely correlated (Table 6; $R^2=0.92$) notably for F-dominated Stations 22 to 30 (60 to >80%) with TChl*a* range of 0.47–1.7 mg m^{-3} at the depth of the F_v/F_m maximum. The correlations between F_v/F_m and σ_{PSII} and the bio-optical parameters TChl*a*/TP, AP/TP, a676/a440 and a490/a676 were all linear (Figure 5; statistics Table 6) though the data set of optical properties at the depth of the F_v/F_m maximum was limited. The relationships between F_v/F_m and the TChl*a*/TP ratio and the optical ratio a676/a440 (Figure 5A&C) and a676/a490 (not shown) were all positive and

https://doi.org/10.1017/S0025315406014287 Published online by Cambridge University Press

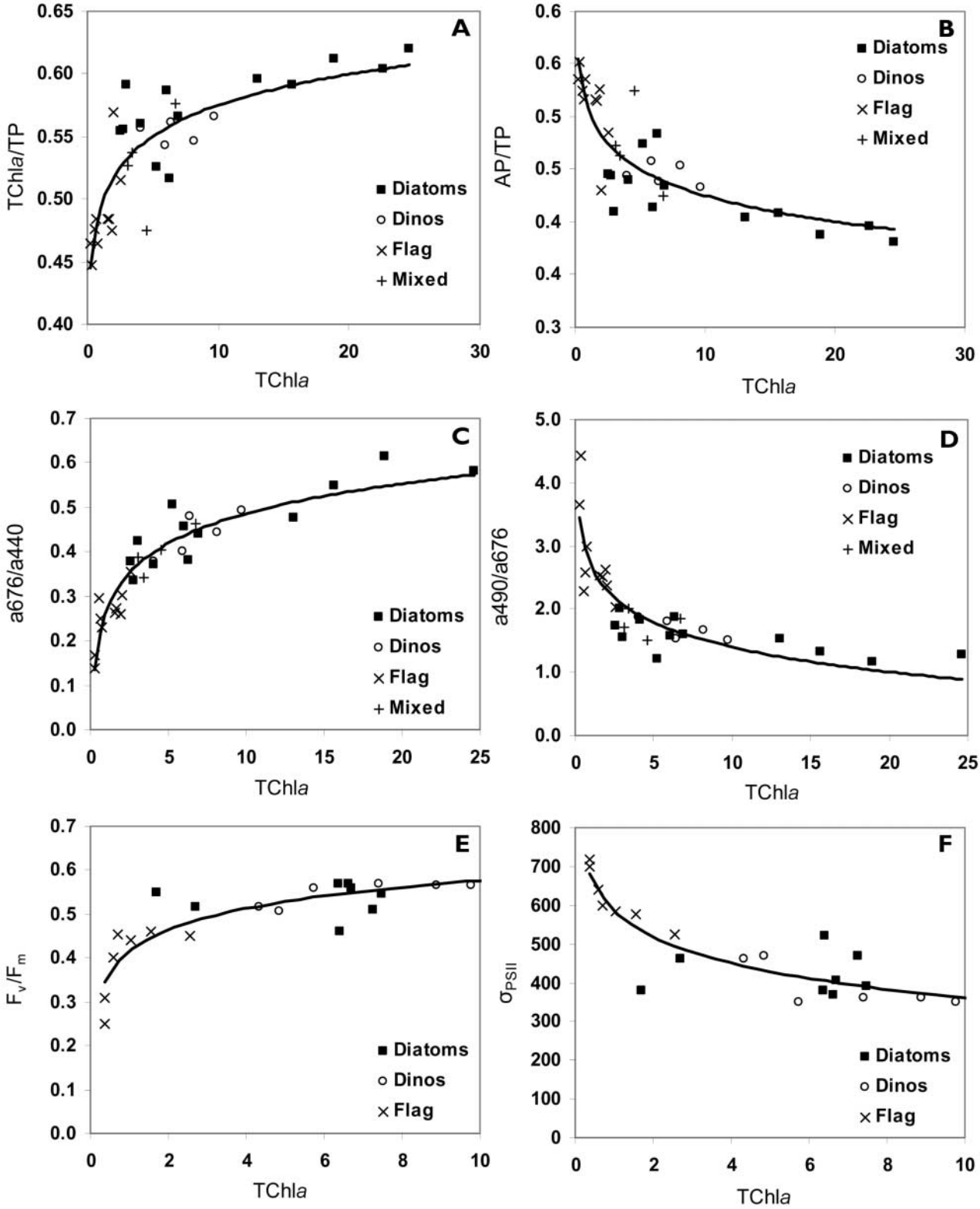

Figure 4. The relationships between TChl*a* (mg m^{-3}) versus (A) TChl*a*/TP; (B) AP/TP; (C) the ratio a676/a440; (D) a490/a676; (E) F_v/F_m; (F) σ_{PSII} ($\times 10^{-20}$ m^2 photon^{-1}). The data points on each figure are identified by the dominant taxa at that station, A–D are for the surface layer data set (Table 2) and E&F are for the F_v/F_m maximum data set (Table 3). Regression equations and statistics are shown in Table 5.

showed the typical split of flagellate dominated stations from the others, whereas the relationships between TChl*a*/TP and a676/a440 (Figure 5B&D) versus σ_{PSII} were negative; σ_{PSII} was positively correlated with AP/TP and a490/a676 (Figures 5E&F). The pigment ratios (TChl*a*/TP, AP/TP) and their optical analogues (a676/a440, a490/a676) were significantly correlated (Figure 5G&H; Table 6).

https://doi.org/10.1017/S0025315406014287 Published online by Cambridge University Press

Table 5. *Regression statistics for the pigment relationships with pigment ratios, optical absorption ratios and the photosynthetic parameters F_v/F_m and σ_{PSII}.*

Independent variable	Dependent variable	Group	Type of relationship	Slope	Intercept	R^2	N
TChl*a*	TChl*a*/TP	All	Log	0.036	0.493	0.71	32
TChl*a*	TChl*a*/TP	Flag.	Linear	0.029	0.451	0.46	10
TChl*a*	TChl*a*/TP	D, d & M	Linear	0.004	0.532	0.47	22
TP	TChl*a*/TP	All	Log	0.037	0.468	0.66	32
TP	TChl*a*/TP	Flag.	Linear	0.013	0.454	0.35	10
TP	TChl*a*/TP	D, d & M	Linear	0.002	0.531	0.42	22
TChl*a*	AP/TP	All	Log	−0.036	0.507	0.71	32
TChl*a*	a_{676}/a_{440}	All	Log	0.097	0.264	0.88	31
TChl*a*	a_{676}/a_{440}	Flag.	Log	0.065	0.256	0.68	10
TChl*a*	a_{676}/a_{440}	D, d & M	Log	0.105	0.252	0.76	21
TChl*a*	a_{676}/a_{490}	All	Log	0.126	0.397	0.81	31
TChl*a*	a_{676}/a_{490}	Flag.	Log	0.077	0.381	0.63	10
TChl*a*	a_{676}/a_{490}	D, d & M	Log	0.128	0.399	0.57	21
TChl*a*	a_{490}/a_{676}	All	Log	−0.564	2.695	0.79	31
TChl*a*	a_{490}/a_{676}	Flag.	Log	−0.697	2.770	0.61	10
TChl*a*	a_{490}/a_{676}	D, d & M	Log	−0.262	2.104	0.47	21
TChl*a*	F_v/F_m	All	Log	0.070	0.415	0.75	21
TP	F_v/F_m	All	Log	0.075	0.363	0.72	21
TChl*a*	σ_{PSII}	All	Log	−97.8	586.3	0.80	21
AP	σ_{PSII}	All	Log	−110.7	585.7	0.73	21

Table 6. *Regression statistics for the inter-relationships between the pigment ratios, optical absorption ratios and the photosynthetic parameters F_v/F_m and σ_{PSII}.*

Independent variable	Dependent variable	Group	Type of relationship	Slope	Intercept	R^2	N
F_v/F_m	σ_{PSII}	All	Linear	−1291	1114	0.92	21
TChl*a*/TP	F_v/F_m	All	Linear	1.537	−0.328	0.79	21
TChl*a*/TP	F_v/F_m	Flag.	Linear	2.695	−0.878	0.66	7
TChl*a*/TP	F_v/F_m	D, d & M	Linear	0.697	0.147	0.26	14
TChl*a*/TP	σ_{PSII}	All	Linear	−2100	1599	0.81	21
TChl*a*/TP	σ_{PSII}	Flag.	Linear	−2424	1766	0.75	7
TChl*a*/TP	σ_{PSII}	D, d & M	Linear	−809.7	865.1	0.13	14
a_{676}/a_{440}	F_v/F_m	All	Linear	0.688	0.224	0.80	11
a_{676}/a_{440}	σ_{PSII}	All	Linear	−1136	932.6	0.81	11
a_{490}/a_{676}	σ_{PSII}	All	Linear	0.003	0.550	0.81	11
AP/TP	σ_{PSII}	All	Linear	2099	−501	0.79	21
AP/TP	σ_{PSII}	Flag.	Linear	2425	−658.5	0.75	7
AP/TP	σ_{PSII}	D, d & M	Linear	809.7	55.3	0.13	14
TChl*a*/TP	a_{676}/a_{440}	All	Linear	1.995	−0.688	0.70	31
TChl*a*/TP	a_{676}/a_{440}	Flag.	Linear	1.265	−0.363	0.46	10
TChl*a*/TP	a_{676}/a_{440}	D, d & M	Linear	1.386	−0.333	0.38	21
AP/TP	a_{490}/a_{676}	All	Linear	11.55	−3.35	0.62	31
AP/TP	a_{490}/a_{676}	Flag.	Linear	12.86	−3.81	0.37	10
AP/TP	a_{490}/a_{676}	D, d & M	Linear	2.811	0.390	0.15	21

We observed that: small cells (flagellates) had the lowest biomass (0.26–1.9 mg m^{-3}), TChl*a*/TP (0.45–0.52), a676/a440 (0.14–0.35), F_v/F_m (0.25–0.46) and highest range of σ_{PSII} (525–720). Larger cells, diatoms and dinoflagellates overlapped in range. Diatoms had the highest biomass (2.5 to 24.6 mg m^{-3}), highest TChl*a*/TP (0.52–0.62), a676/a440 (0.34–0.62), F_v/F_m (0.4–0.57) and a lower value range of σ_{PSII} (370–520). There were no F_v/F_m and σ_{PSII} data at the high chlorophyll diatom dominated stations, so the data shown do not represent the full range of these parameters. Dinoflagellates had a limited biomass range (4 to 9.7 mg m^{-3}), intermediate values for TChl*a*/TP (0.54–0.57), a676/a440 (0.38–0.49), F_v/F_m (0.52–0.57) and the lowest value range of σ_{PSII} (350–470).

https://doi.org/10.1017/S0025315406014287 Published online by Cambridge University Press

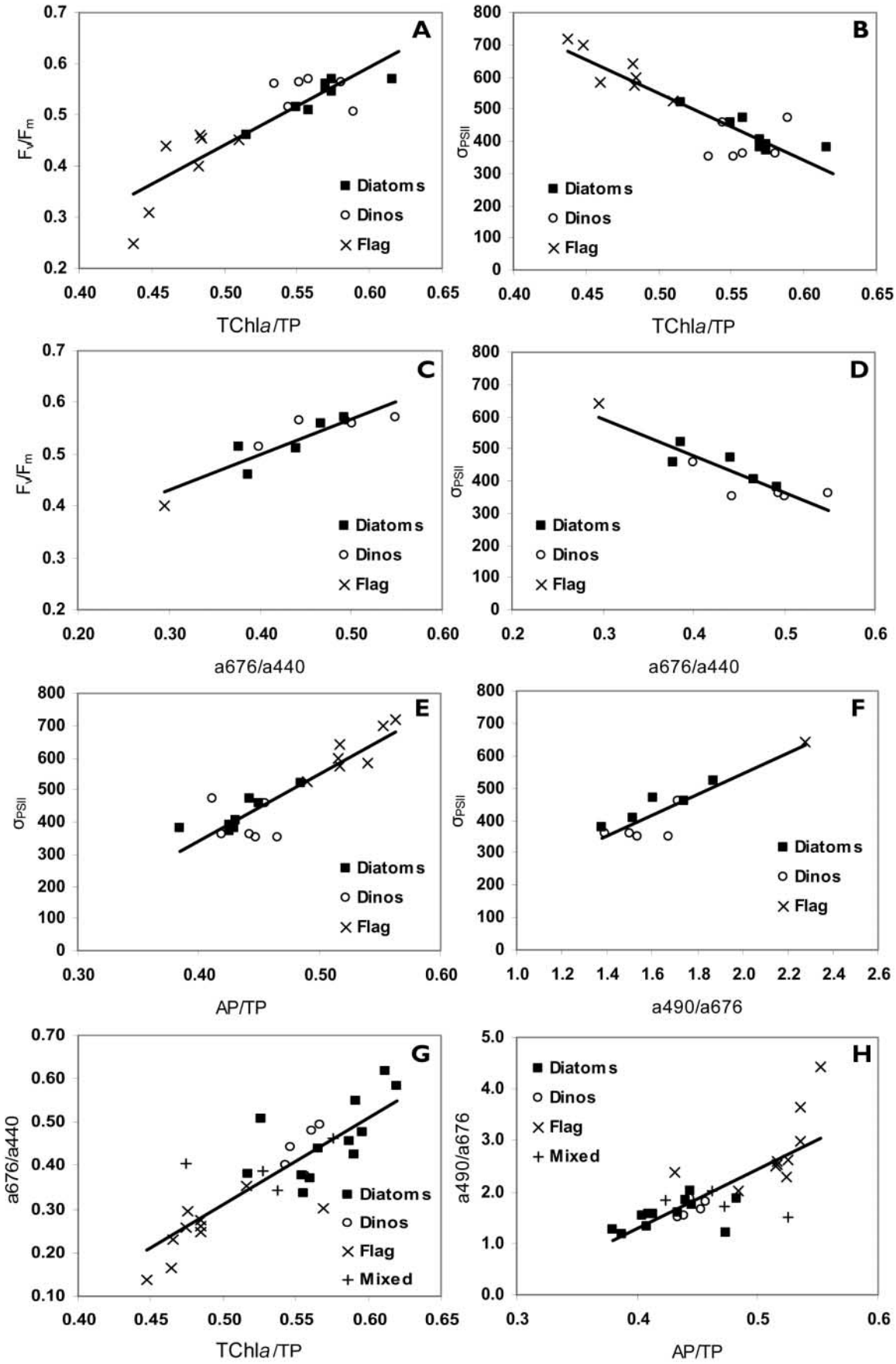

Figure 5. Relationships for: (A&B) TChl*a*/TP versus F_v/F_m and σ_{PSII} ($\times 10^{-20}$ m^2 photon^{-1}); (C&D), showing the absorption ratio a676/a440 versus F_v/F_m and σ_{PSII} ($\times 10^{-20}$ m^2 photon^{-1}); (E) AP/TP versus σ_{PSII} ($\times 10^{-20}$ m^2 photon^{-1}); (F) a490/a676 versus σ_{PSII} ($\times 10^{-20}$ m^2 photon^{-1}); (G) TChl*a*/TP versus a676/a440; and (H) AP/TP versus a490/a676. A–F use the F_v/F_m maximum data set (Table 3) and G&H use the surface layer data set (Table 2). The data points on each figure are identified by the dominant taxa at that station and the regression equations and statistics are shown in Table 6.

https://doi.org/10.1017/S0025315406014287 Published online by Cambridge University Press

DISCUSSION

A diverse data set of bio-optical properties from the upwelling, nutrient-rich, eutrophic, Benguela ecosystem and the offshore mesotrophic area have been analysed for correlations (functional relationships) and characteristic properties associated with the dominant PFTs (diatom, dinoflagellate or small flagellates) observed at discrete stations. Diatoms and dinoflagellates (TChl*a* range >2.0 to $25\,mg\,m^{-3}$) dominated the on-shelf nutrient-rich stations in recently upwelled water with temperature ranging between 12°C and 15°C. Nitrates were close to depletion at a few stations in and around St Helena Bay and silicates were never near depletion. It would seem that in this dynamic upwelling region at this time, the re-supply of nutrients was sufficient to avoid depletion, and with moderate F_v/F_m ($\sim$0.51) it would seem unlikely that phytoplankton growth was limited. Flagellates were most abundant offshore (SST >16°C) where NO_3 levels were low (generally $<1\,\mu M$) and silicate abundant (1.7–7.1 μM) but with low values of F_v/F_m (0.25–0.31). The distribution of PFTs agreed with the conclusions of Mitchell-Innes & Pitcher, 1992, that dominant taxa in the Benguela ecosystem were determined by the water temperature and chlorophyll concentrations. We observed that each PFT (diatoms, dinoflagellates and flagellates) had different physiological characteristics that were exploited during the developing chronology of the upwelling cycle, but it was not clear if the community structure was defined by the nitrate levels as suggested by Barlow et al., 2004. In N-limitation, phytoplankton have been shown to increase light harvesting pigments in relation to reaction centre proteins and reduce the number of PSII reaction centres in relation to the light harvesting complex (Kolber et al., 1988; Falkowski et al., 1989; Geider et al., 1993; Berges et al., 1996). This resulted in an increased σ_{PSII} and light harvesting with the energy funnelled to a smaller number of PSII reaction centres. Flagellates in nitrate-limited conditions have larger σ_{PSII} than diatoms, which thrive in high nitrate waters. The low F_v/F_m in the flagellate dominated stations is consistent with this, as F_v/F_m is a measure of the functional PSII reaction centres and these are reduced in N-limited conditions (Kolber et al., 1988).

As has been observed in many other ecosystems (Aiken et al., 1995, 2004; Trees et al., 2000) TChl*a* had a robust relationship with TP, AP and AC; R^2 was >0.96 to $\sim$0.99. In this study we observed that the relationship for the flagellate dominated populations differed from the others (M+D+d populations). Pigment ratios (e.g. TChl*a*/TP) were not constant (ranging from 0.45 to 0.62) but increased with increasing TChl*a*; again the flagellate group was lower than the other groups (M+D+d), which is consistent with the first observation. The highly significant TChl*a*/TP to TChl*a* and F_v/F_m to TChl*a* relationships validate the hypothesis that phytoplankton synthesize Chl*a* preferentially in conditions conducive to growth (surplus nutrients and adequate light). A taxonomic preference was shown for flagellates in low nutrient, higher temperature regimes and for diatoms in high nutrient, lower temperature regimes. There are separate and significant relationships for the flagellate and the other groups suggesting that this process is general and independent of taxonomic groupings. This conclusion is consistent with the high energy requirement of Chl*a* synthesis and maintenance and that plants readily de-synthesize Chl*a* when growth conditions are unfavourable (Margalef, 1967). The alternative hypothesis, that plants synthesize AP preferentially when light, nutrients and photosynthesis are limited, is logically perverse. The observed linear correlations between TChl*a*/TP and F_v/F_m (this study and Aiken et al., 2004) provide additional support for the hypothesis: phytoplankton with a higher fraction of Chl*a* had higher rates of photosynthetic quantum efficiency. The iron enrichment experiments IronExII (Behrenfeld et al., 1996) and SOIREE (Boyd & Abraham, 2001), also showed significant correlations between TChl*a*/TP and F_v/F_m (J. Aiken, unpublished data). In this study there was a clear relationship between the increase in TChl*a* and the increasing proportion of TChl*a* as a fraction of the total pigments (TChl*a*/TP) over the limited range $0.26–1.9\,mg\,m^{-3}$ within the flagellate group (that comprised chrysophytes, prymnesiophytes, cryptophytes and chlorophytes). This provided compelling evidence that the Chl*a*-synthesis process was dominant over the taxonomic selection; prymnesiophytes (hex-specific) were the dominant taxa for the F-dominated stations, indicating that there was no taxonomic shift that might annul this argument.

Distinctly different bio-optical characteristics were observed for different PFTs, providing a separation of three taxonomic groups on the basis of key bio-optical properties: pigment relationships (TChl*a* to TP, AP to TP), pigment ratios (e.g. TChl*a*/TP, AP/TP), optical ratios (e.g. a676/a440, a676/a490) and photosynthetic parameters (F_v/F_m and σ_{PSII}). The variation of TChl*a*/TP and the optical analogue a676/a440, both strongly correlated with F_v/F_m and σ_{PSII} (inversely), provided evidence of a relationship between photosynthesis (these parameter values) and ocean colour (the optical signature of ocean waters observed *in situ* or remotely). We conclude that colour change brought about by the strong blue absorption of TChl*a* at 400–470 nm, is the pre-eminent cause of change in ocean colour spectra.

This study showed that the physiological parameters, F_v/F_m and σ_{PSII} had different ranges for different PFTs, concurring with laboratory studies that taxonomic variability was greater than variability at the level of cellular physiology (Suggett et al., 2004). Moore et al., 2005 arrived at a similar conclusion for data from the north-east Atlantic. From this data set it has been shown that TChl*a*/TP, a676/a440, F_v/F_m and σ_{PSII} had robust inter-relationships, allowing the discrimination of bio-optical properties for three dominant PFTs: diatoms, dinoflagellates and flagellates. The ranges of these four parameters can be explained partially by the percentage of PFT dominance at each station. On this basis it should be possible to allocate percentages of the TChl*a* and TP to each PFT, using mixing models. Further research is required to confirm the application of these functional processes in other ecosystems and across the globe generally.

The authors thank the officers and crew of the FRS 'Africana' for their wholehearted support that contributed greatly to the success of the cruise. Thanks to S. Weeks and C. Whittle of OceanSpace CC, University of Cape Town, for processing

https://doi.org/10.1017/S0025315406014287 Published online by Cambridge University Press

SeaWiFS data and transmitting images to the ship daily. C. Duncombe Rae, M. van den Berg, and C. Boucher provided support with the archiving and processing of hydrographic data. We thank ESA and NASA for their funding support for this cruise.

REFERENCES

Aiken, J., Fishwick, J.R., Moore, G.F. & Pemberton, K., 2004. The annual cycle of phytoplankton photosynthetic quantum efficiency, pigment composition and optical properties in the western English Channel. *Journal of the Marine Biological Association of the United Kingdom*, **84**, 301–313.

Aiken, J., Moore, G.F., Trees, C.C., Hooker, S.B. & Clark, D.K., 1995. The SeaWiFS CZCS-type pigment algorithm. *NASA Technical Memorandum 104566* (ed. S.B. Hooker and E.R. Firestone). *SeaWiFS Technical Report Series*, **29**, 32 pp.

Aiken, J. et al., 2000. The Atlantic Meridional Transect: overview and synthesis of data. *Progress in Oceanography*, **45**, 257–312.

Alvain, S., Moulin, C., Dandonneau, Y. & Bréon, F.M., 2005. Remote sensing of phytoplankton groups in case 1 waters from global SeaWiFS imagery. *Deep-Sea Research I*, **52**, 1989–2004.

Barlow, R.G., Aiken, J., Moore, G.F., Holligan, P.M. & Lavender, S., 2004. Pigment adaptations in surface phytoplankton along the eastern boundary of the Atlantic Ocean. *Marine Ecology Progress Series*, **281**, 13–26.

Barlow, R.G., Cummings, D.G. & Gibb, S.W., 1997. Improved resolution of mono- and Divinyl chlorophylls a and b and Zeaxanthin and Lutein in phytoplankton extracts using reverse phase C-8 HPLC. *Marine Ecology Progress Series*, **161**, 303–307.

Behrenfeld, M.J., Bale, A.J., Kolber, Z., Aiken, J. & Falkowski, P.G., 1996. Iron availability limits nutrient utilization in the Eastern Equatorial Pacific Ocean. *Nature, London*, **383**, 508–511.

Behrenfeld, M.J. & Falkowski, P.G., 1997. Photosynthetic rates derived from satellite-based chlorophyll concentrations. *Limnology and Oceanography*, **42**, 1–20.

Berges, J.A., Charlebois, D.O., Mauzerall, D.C. & Falkowski, P.G., 1996. Differential effects of nitrogen limitation on photosynthetic efficiency of photosystems I and II in microalgae. *Plant Physiology*, **110**, 689–696.

Bidigare, R.R., Ondrusek, M.E., Morrow, J.H. & Kiefer, D.A., 1990. *In vivo* absorption properties of algal pigments. *SPIE Ocean Optics*, **1302**, 290–302.

Blackford, J.C., Allen, J.I. & Gilbert, F.G., 2004. Ecosystem dynamics at six contrasting sites: a generic modelling study. *Journal of Marine Systems*, **52**, 191–215.

Boyd, P.W. & Abraham, E.R., 2001. Iron-mediated changes in phytoplankton photosynthetic competence during SOIREE. *Deep-Sea Research*, **48**, 2529–2550.

Bricaud, A.L. & Stramski, D., 1990. Spectral absorption coefficients of living phytoplankton and nonalgal biogenous matter: a comparison between the Peru upwelling area and Sargasso Sea. *Limnology and Oceanography*, **35**, 562–582.

Cullen, J.J. & Davis, R.F., 2003. The blank can make a big difference in oceanographic measurements. *Limnology and Oceanography Bulletin*, **12**, 29–35.

Falkowski, P.G., Sukenik, A. & Herzig, R., 1989. Nitrogen limitation in *Isochrysis Galbana* (Haptophyceae). II. Relative abundance of chloroplast proteins. *Journal of Phycology*, **25**, 471–478.

Fasham, M.R.J., 1993. Modelling the marine biota. In *The global carbon cycle* (ed. M. Heimann), pp. 457–504. Berlin: Springer.

Flynn, K.J., 2001. A mechanistic model for describing dynamic multi-nutrient, light, temperature interactions in phytoplankton. *Journal of Plankton Research*, **9**, 977–997.

Geider, R.J., La Roche, J., Greene, R.M. & Olaizola, M., 1993. Response of the photosynthetic apparatus of *Phaeodactylum Tricornutum* (Bacillariophyceae) to nitrate, phosphate, or iron starvation. *Journal of Phycology*, **29**, 755–766.

Geider, R.J., MacIntyre, H.L. & Kana, T.M., 1997. A dynamic model of phytoplankton growth and acclimation: responses of the balanced growth rate and the chlorophyll-a: carbon ratio to light, nutrient limitation and temperature. *Marine Ecology Progress Series*, **148**, 187–200.

Grasshoff, K., Ehrhardt, M. & Kremling, K., 1983. *Methods of seawater analysis*, 2nd edn. Weinheim: Verlag Chemie.

Gregg, W.W., Ginoux, P., Schopf, P.S. & Casey, N.W., 2003. Phytoplankton and iron: validation of a global three-dimensional ocean biogeochemical model. *Deep-Sea Research II*, **50**, 3143–3169.

Hardman-Mountford, N.J., Richardson, A.J., Agenbag, J.J., Hagen, E., Nykjaer, L., Shillington, F.S. & Villacastin, C., 2003. Ocean climate of the South East Atlantic observed from satellite data and wind models. *Progress in Oceanography*, **59**, 181–221.

Heath, M.R., Richardson, K. & Kiorboe, T., 1990. Optical assessment of phytoplankton nutrient depletion. *Journal of Plankton Research*, **12**, 381–396.

Holmboe, N., Jensen, H.S. & Andersen, F.O., 1999. Nutrient addition bioassays as indicators of nutrient limitation of phytoplankton in a eutrophic estuary. *Marine Ecology Progress Series*, **186**, 95–104.

Jeffrey, S.W. & Hallegraeff, G.M., 1980. Studies of phytoplankton species and photosynthetic pigments in a warm core eddy of the East Australian current. II. A note on pigment methodology. *Marine Ecology Progress Series*, **3**, 295–301.

Kirkwood, D.S., 1994. *The SAN plus segmented flow analyser: seawater analysis*. Lowestoft, UK: Ministry of Agriculture, Fisheries and Food (MAFF). [Publication no. 07300194.]

Kishino, M., Okami, N. & Ichimura, S., 1985. Estimation of the spectral absorption coefficients of phytoplankton in the sea. *Bulletin of Marine Science*, **37**, 634–642.

Kolber, Z. & Falkowski, P.G., 1993. Use of active fluorescence to estimate phytoplankton photosynthesis *in situ*. *Limnology and Oceanography*, **38**, 1646–1665.

Kolber, Z.S., Prasil, O. & Falkowski, P.G., 1998. Measurments of variable fluorescence using fast repetition rate techniques: defining methodology and experimental protocols. *Biochima et Biophysica Acta*, **1367**, 88–106.

Kolber, Z., Zehr, J. & Falkowski, P.G., 1988. Effects of growth irradiance and nitrogen limitation on photosynthetic energy conversion in photosystem II. *Plant Physiology*, **88**, 923–929.

Le Quéré, C. et al., 2005. Ecosystem dynamics based on plankton functional types for global ocean biogeochemistry models. *Global Change Biology*, **11**, 2016–2040.

Margalef, R., 1967. Some concepts relative to the organization of plankton. *Oceanography and Marine Biology. Annual Review*, **5**, 257–289.

Mitchell, B.G. & Kiefer, D.A., 1988. Chlorophyll a specific absorption and fluorescence excitation spectra for light limited phytoplankton. *Deep Sea Research*, **35**, 639–663.

Mitchell-Innes, B.A. & Pitcher, G.C., 1992. Hydrographic parameters as indicators of the suitability of phytoplankton populations as food for herbivorous copepods. *South African Journal of Marine Science*, **12**, 355–365.

Mitchell-Innes, B.A. & Winter, A., 1987. Coccolithophores: a major phytoplankton component in mature upwelled waters off the Cape Peninsula, South Africa in March 1983. *Marine Biology*, **95**, 25–30.

Moore, C.M. et al., 2003. Physical controls on phytoplankton physiology and production at a shelf sea front: a fast repetition rate fluorometer based field study. *Marine Ecology Progress Series*, **259**, 29–45.

https://doi.org/10.1017/S0025315406014287 Published online by Cambridge University Press

Moore, C.M., Lucas, M.I., Sanders, R. & Davidson, R., 2005. Basin-scale variability of phytoplankton bio-optical characteristics in relation to bloom state and community structure in the Northeast Atlantic. *Deep-Sea Research I*, **52**, 401–419.

Morel, A., 1991. Light and marine photosynthesis: a spectral model with geochemical and climatological implications. *Progress in Oceanography*, **26**, 263–306.

Pitcher, G.C., Boyd, A.J., Horstman, D.A. & Mitchell-Innes, B.A., 1998. Subsurface dinoflagellate populations, frontal blooms and the formation of red tide in the southern Benguela upwelling system. *Marine Ecology Progress Series*, **172**, 253–264.

Pitcher, G.C., Brown, P.C. & Mitchell-Innes, B.A., 1992. Spatio-temporal variability of phytoplankton in the southern Benguela upwelling system. *South African Journal of Marine Science*, **12**, 439–456.

Platt, T., 1986. Primary production of the ocean water column as a function of surface light intensity: models for remote sensing. *Deep-Sea Research*, **33**, 149–163.

Sathyendranath, S., Watts, L., Devred, E., Platt, T., Caverhill, C. & Maass, H., 2004. Discrimination of diatoms from other phytoplankton using ocean colour data. *Marine Ecology Progress Series*, **272**, 59–68.

Schluter, L., Riemann, B. & Sondergaard, M., 1997. Nutrient limitation in relation to phytoplankton carotenoid chlorophyll a ratios in freshwater mesocosms. *Journal of Plankton Research*, **19**, 891–906.

Smyth, T.J., Pemberton, K.L., Aiken, J. & Geider, R.J., 2004. A methodology to determine primary production and phytoplankton photosynthetic parameters from fast repetition rate fluorometry. *Journal of Plankton Research*, **26**, 1–15.

Suggett, D., Kraay, G., Holligan, P., Davey, M., Aiken, J. & Geider, R., 2001. Assessment of photosynthesis in a spring cyanobacterial bloom by use of fast repetition rate fluorometer. *Limnology and Oceanography*, **46**, 802–810.

Suggett, D.J., MacIntyre, H.L. & Geider, R.J., 2004. Evaluation of biophysical and optical determinations of light absorption by photosystem II in phytoplankton. *Limnology and Oceanography Methods*, **2**, 316–332.

Suggett, J.D., Moore, C.M., Maranon, E., Omachi, C., Varela, R.A., Aiken, J. & Holligan, P.M., 2006. Photosynthetic electron turnover in the tropical and subtropical Atlantic Ocean. *Deep Sea Research*, in press.

Trees, C.C., Clark, D.K., Bidigare, R.R., Ondrusek, M.E. & Muller, J.L., 2000. Accessory pigments versus chlorophyll a concentrations within the euphotic zone: a ubiquitous relationship. *Limnology and Oceanography*, **45**, 1130–1143.

Vidussi, F., Claustre, H., Manaca, B.B., Luchetta, A. & Marty, J.-C., 2001. Phytoplankton pigment distribution in relation to upper thermocline circulation in the eastern Mediterranean Sea during winter. *Journal of Geophysical Research*, **106**, 19939–19956.

Submitted 31 March 2006. Accepted 23 October 2006.

https://doi.org/10.1017/S0025315406014287 Published online by Cambridge University Press